Molecular Crystals
Publication details, including instructions for authors and subscription information:
http://www.tandfonline.com/loi/gmcl15

Long Range Order and Thermal Fluctuations in Liquid Crystals

P. G. De Gennes [a]

[a] Laboratoire de Physique des Solides Faculté des Sciences, 91, Orsay, France

Version of record first published: 29 Aug 2007.

To cite this article: P. G. De Gennes (1969): Long Range Order and Thermal Fluctuations in Liquid Crystals, Molecular Crystals, 7:1, 325-345

To link to this article: http://dx.doi.org/10.1080/15421406908084881

Molecular Crystals and Liquid Crystals. 1969. Vol. 7, pp. 325–345

Printed in Great Britain

Long Range Order and Thermal Fluctuations in Liquid Crystals

P. G. DE GENNES

Laboratoire de Physique des Solides‡
Faculté des Sciences
91 — Orsay, France

Abstract—Some recent applications of the Oseen-Zocher-Frank elastic theory of nematic and cholesteric liquid crystals are reviewed.

(1) The effects of a static magnetic field H are calculated in detail. In particular, for a cholesteric system, the spiral structure is distorted by the field and the period increases with H, up to a critical field H_c at which a nematic phase is expected. H_c is inversely proportional to the pitch of the unperturbed helix, and should be observable in systems with long periods. A cholesteric → nematic transition of this type has in fact been qualitatively observed.

(2) The optical striations which are observed when a cholesteric liquid is inserted in a region of variable thickness have been shown by Cano to correspond to discontinuities of the torsion. The transition region between regions of different pitch has been analyzed in terms of a " disclination line " normal to the helical axis.

(3) In a nematic liquid crystal the long wavelength thermal fluctuations of orientation can be analyzed from macroscopic elastic considerations: these large fluctuations are responsible for the strong scattering and depolarization of light measured by Châtelain. The angular dependence of the scattering intensity can thus be explained without any assumption on " swarms ".

1. Introduction

The statistical properties of liquid crystals at the molecular level (e.g. short range order as measured by X-rays) are not well understood. On the other hand, the properties on a larger scale (10^3 Å

‡ Associé au C.N.R.S.

and above) may be analyzed without ambiguity in terms of a continuum theory, of which slightly different variants have been constructed by Oseen[1], Zocher[2] and Frank.[3] This macroscopic description is ideally suited for a study of possible *distortions* of a liquid crystal structure. Such distortions may occur in very different contexts:

(a) they may be induced by weak external forces: in practice, the most satisfactory external agent is a magnetic field H.[4] Orientation under a field H is one efficient way of preparing nematic single crystals. There is in general a competition between the orientation imposed by the walls of the container and the orientation imposed by the field. The latter dominates if the sample dimensions are longer than a certain *coherence length* $\xi(H)$ (inversely proportional to H). This notion emerged very early from experiments by Frederiks[5] and is rederived for completeness in Section 2. We also discuss in Section 2 the effect of a field H on a cholesteric material and the remarkable phase transitions which may occur there.

(b) Distortions may also be imposed by suitable *boundary conditions*, with oriented walls. In Section 3, we analyze such a case, namely the so-called " Grandjean planes " observed in cholesteric crystals included in a slab of variable thickness.[6] We suggest that they correspond in fact not to planes, but to " disclination lines " according to Frank's terminology.[3]

(c) *Spontaneous* distortions are due to thermal agitation. We compute their amplitude in Section 4, and find that it is very large for long (optical) spatial wavelengths. The result is a very strong scattering and depolarization of light, which is indeed observed.[7]

Before entering into these detailed discussions, we shall rewrite the basic equations of the continuum theory,[1,2,3] for nematic and cholesteric crystals. At each point $\mathbf{r}$, the preferred axis of the liquid is described by a unit vector, or " director " $\mathbf{n}(\mathbf{r})$. It is assumed that the molecular dipoles show no ferroelectricity: $\mathbf{n}$ and $-\mathbf{n}$ are fully equivalent states. For a nematic crystal, the most general form of the distortion free energy (per cm^3), is then:

$$F_0 = \tfrac{1}{2}\{\kappa_{11}(\text{div } \mathbf{n})^2 + \kappa_{22}(\mathbf{n} \cdot \text{curl } \mathbf{n})^2 + \kappa_{33}(\mathbf{n} \times \text{curl } \mathbf{n})^2 + \kappa_{24}[(\partial_\alpha \mathbf{n}_\beta)(\partial_\beta \mathbf{n}_\alpha) - (\partial_\alpha \mathbf{n}_\beta)(\partial_\alpha \mathbf{n}_\beta)]\} \quad (1.1)$$

Here $\kappa = x,y,z$, $\partial_\alpha \equiv \partial/\partial x_\alpha$, and a summation is implied on each repeated index. As first noted by Eriksen[3] an integration by parts shows that κ_{24} does not contribute to the volume energies. Thus (leaving aside the question of boundary conditions, to which we shall come back in Section 2.1), we may omit κ_{24} completely, and write:

$$F_0 = \tfrac{1}{2}[\kappa_{11}(\text{div } \mathbf{n})^2 + \kappa_{22}(\mathbf{n} \cdot \text{curl } \mathbf{n})^2 + \kappa_{33}(\mathbf{n} \times \text{curl } \mathbf{n})^2] \quad (1.2)$$

To this distortion energy we have to add a nematic term describing the effects of the magnetic field H. If the susceptibilities $\chi_\parallel$ (for $\mathbf{H} \parallel n$) and $\chi_\perp$ (for $\mathbf{H}$ normal to $\mathbf{n}$) are different, there is a coupling term:

$$F_{\text{mag}} = -\tfrac{1}{2}\chi_a(\mathbf{n} \cdot \mathbf{H})^2 \quad (1.3)$$

where $\chi_a = \chi_\parallel - \chi_\perp \cdot \chi_a$ is a susceptibility per unit volume, and may be positive or negative depending on the shape of the constituent molecules (χ_a is positive for cigar-shaped diamagnetic ellipsoids, and negative for " pancake " ellipsoids). Each of the three constants κ_{11} is of order $k_B T_c/a$ where $k_B T_c$ is a typical intermolecular interaction energy, and a is a molecular diameter.

How does the structure (1.2) change for cholesteric systems? It may be worthwhile to point out at this stage that spiral structures might occur in two very different situations:

(a) with molecules which are *not* optically active, spirals are still allowed on symmetry grounds: in magnetic materials the interactions are parity-invariant, but spirals do occur (they grow right- or left-handed at random). A plot energy versus spiral wave vector $q = \partial\theta/\partial z$ for such a case is symmetric but, as shown on Fig. 1a, it may show minima at non 0 q's. However, calculations on magnetic systems[8] suggest that such minima occur only if the forces between *next nearest* neighbor molecules are important. This is not expected to happen with the Van der Waals forces of interest here, and in fact we do not know of any existing examples of this type.

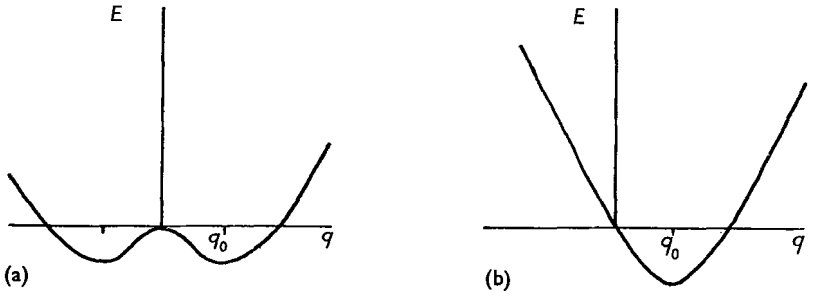

Figure 1. Plot of energy versus spiral wave vector for two possible types of cholesterics: Fig. 1a corresponds to molecules which coincide with their mirror image. Spiral structures could occur in this case if forces between second neighbor molecules were important. Fig. 1b corresponds to the usual case, where the constituent molecules are optically active.

(b) with optically active constituents, the plot of energy versus q becomes asymmetric as shown on Fig. 1b and the minimum is necessarily shifted to some non 0 value of q ($q = q_0$). Since the differences between the right- and left-handed species are often rather small, q_0 is small on the molecular scale ($q_0 a \ll 1$). This allows to apply the macroscopic description of Eq. (1.2) even for wave vectors comparable to q_0.

In these conditions, the distortion free energy becomes

$$F_0 = \tfrac{1}{2}[\kappa_{11}(\text{div } \mathbf{n})^2 + \kappa_{22}(\mathbf{n} \cdot \text{curl } \mathbf{n} + q_0)^2 + \kappa_{33}(\mathbf{n} \times \text{curl } \mathbf{n})^2] \quad (1.4)$$
(cholesteric)

Minimizing the overall free energy

$$\mathscr{F} = \int d\tau (F_0 + F_{\text{mag}})$$

with the constraint $n^2 = 1$, one can write down the bulk equilibrium equations. We shall do this directly on the examples to be discussed below. These equations must be supplemented by boundary conditions:

(a) if the wall is a single crystal, the interface being a simple crystallographic plane (a cleavage plane), there will be one (or at most a few equivalent) preferred directions of $\mathbf{n}$ at the surface, with respect to the crystal axes.

(b) with less ideal surfaces the situation is in general complex. The most reproducible boundary conditions are obtained by the polishing method of Châtelain.[7] In this case **n**, at the surface, must be parallel to the polishing direction.

(c) at a liquid crystal-air interface, the only quantity which is fixed is the angle θ between **n** and the interface. The boundary condition may be of the form $\theta = 0$, or $\theta = \pi/2$ (or even $\theta = \theta_0$, although there does not seem to be clear cut examples of this case).

We shall now discuss some specific applications of these notions.

2. Magnetic Field Effects

1. Alignment by a Field in a Nematic System

Consider a nematic crystal occupying the half space $x > 0$ as shown on Fig. 2a. The wall (in the yz plane) imposes a preferred direction $\pm 0z$. We assume that the anisotropic part of the susceptibility $\chi_a = \chi_\parallel - \chi_\perp$ is *positive* and we put a magnetic field in the y direction. Far from the wall **n** will certainly become parallel to **H**. But near the wall there is a transition layer, in which **n** undergoes a *torsion*:

$$n_y = \cos \phi(x) \qquad (2.1)$$
$$nz = \sin \phi(x)$$

The free energy $\mathscr{F}$ (per cm^2 of the wall) is, according to (1.1) ($\simeq$ 0.2):

$$\mathscr{F} = \frac{1}{2}\int_0^\infty dx \left[\kappa_{22}\left(\frac{\partial \phi}{\partial x}\right)^2 - \chi_a H^2 \cos^2 \phi\right] \qquad (2.2)$$

Minimizing this with respect to ϕ we obtain the equilibrium condition

$$-\xi_2^2 \frac{\partial^2 \phi}{\partial x^2} + \sin \phi \cos \phi = 0 \qquad (2.3)$$

where we have introduced a "coherence length" ξ_2 by the equation

$$\xi_2 = \left(\frac{\kappa_{22}}{\chi_a}\right)^{1/2} \frac{1}{H} \qquad (2.4)$$

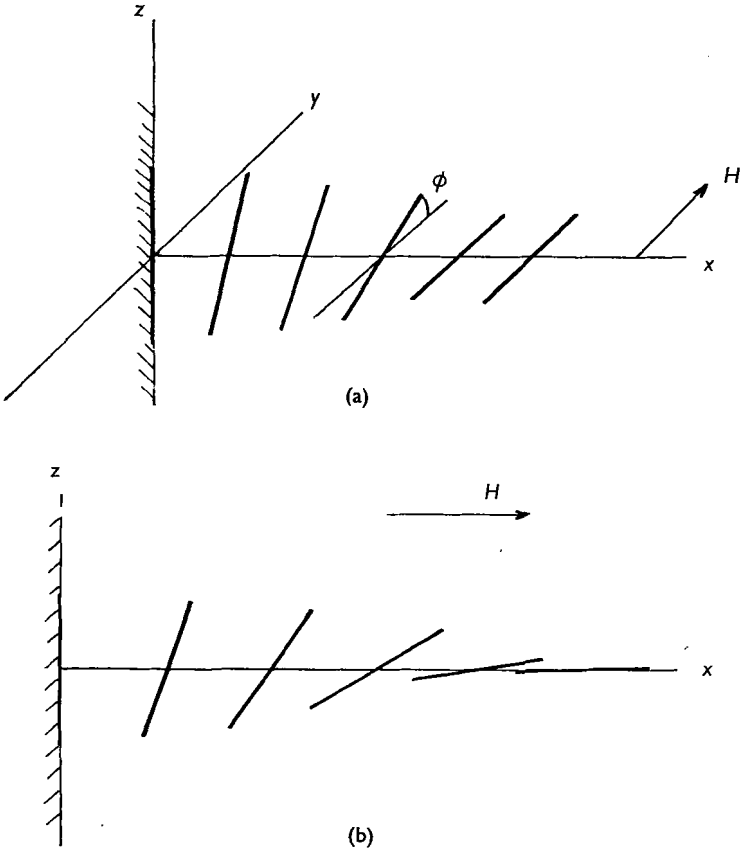

Figure 2. Conformations of a nematic crystal in the vicinity of a uniaxially polished wall. The orientation far in the liquid is imposed by a magnetic field, while the orientation at the boundary is imposed by the wall. The transition between these two limits takes place in one " coherence length " $\xi(H)$. Case (a) corresponds to pure torsion, while case (b) is a mixture of flexion and splay.

Typically both κ_{22} and χ_a are of order 10^{-6} CGS units and ξ_2 is of order one micron for a field of 10^4 oerstedts. Eq. (2.3) is readily integrated to give

$$\tan(\phi/2) = \exp(-X/\xi_2) \tag{2.5}$$

This shows that ξ_2 is the thickness of the transition layer: when

the sample is much thicker than ξ_2, most of the volume is aligned in the field direction.

We have assumed in this calculation that **n** remained strictly parallel to Oz at the surface, even in the presence of the field: this is not entirely obvious, and will be discussed now. The torque (per unit area) which one part of the fluid (say $x > x_0$) exerts on the other ($x < x_0$) is $[\kappa_{22}\,\partial\phi/\partial x]x_0$ and is of order $\kappa_2/\xi_{22} \sim k_B T_c/a\xi_2$. On the other hand, if the boundary is for instance an ideal cleavage plane, the torque (per cm^2) which would be required to pull **n** out of its preferred direction is of atomic size, i.e. of order $k_B T_c/a^2$. Thus the assumption of fixed **n** at the surface is valid in this case, provided that $\xi_2 \gg a$. (The case of a glass wall polished by Châtelain's method is less obvious, since little is known concerning the size of the surface patterns produced by polishing.)

Similar considerations on the alignment by a field can be carried out for other geometries, such as that of Fig 2b where the transition layer carries a deformation which is a combination of

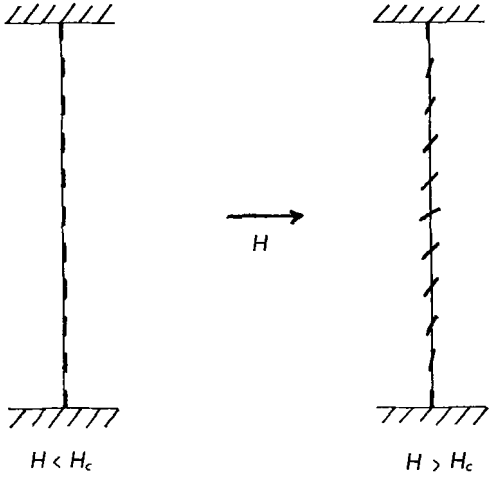

Figure 3. The two possible configurations of a nematic system under a field in the geometry of Frederiks.[5] The molecules at both boundaries are assumed to be normal to the slab.

" flexion " and " splay " in Frank's notation.[3] The calculation is more complex since two elastic constants (κ_{11} and κ_{33}) come into play.[2] The geometry considered by Frederiks[5] is also shown on Fig 3. Here, at a certain threshold field H_c, there is a transition between two configurations.[5a]

But in all these cases we can qualitatively describe the situation by a coherence length

$$\xi = \left(\frac{\chi_a}{K}\right)^{1/2} \frac{1}{H} \tag{2.6}$$

where K is some average of the elastic constants. For instance in the Frederiks experiment the critical field H_c is such that $\xi(H_c) = \alpha d$ where d is the slab thickness and α a numerical constant: this results from purely dimensional analysis, and is in agreement with the experimental data. We shall also in Section 4 study the role played by the coherence length in the spontaneous fluctuations of a nematic structure under fields.

2. Distortion of a Cholesteric Structure by a Field H

The effects of a magnetic field on a cholesteric liquid crystal depend critically on the sign of the susceptibility constant $\chi_a = \chi_\parallel - \chi_\perp$.

(a) If χ_a is *negative*, the director $\mathbf{n}$ tends to lie normal to $\mathbf{H}$. This is realized without any energy expense if the wave vector $\mathbf{a}_0$ of the cholesteric spiral becomes parallel to $\mathbf{H}$. Thus, when $\chi_a < 0$, the field may serve to produce monodomain spirals, but it introduces no distortion of the structure.

(b) If χ_a is *positive*, $\mathbf{n}$ tends to be parallel to $\mathbf{H}$. This situation offers more possibilities; it is discussed in ref. 9 and 10. Clearly in low fields the spiral is essentially undistorted, but tends to have its axis normal to H (Fig. 4a). At higher fields the spiral is deformed (Fig. 4b, c). The change of pitch with field is shown on Fig. 5. Finally, one reaches a nematic structure at a critical field:

$$H_c = \frac{\pi}{2}\left(\frac{\kappa_{22}}{\chi_a}\right)^{1/2} q_0 \tag{2.7}$$

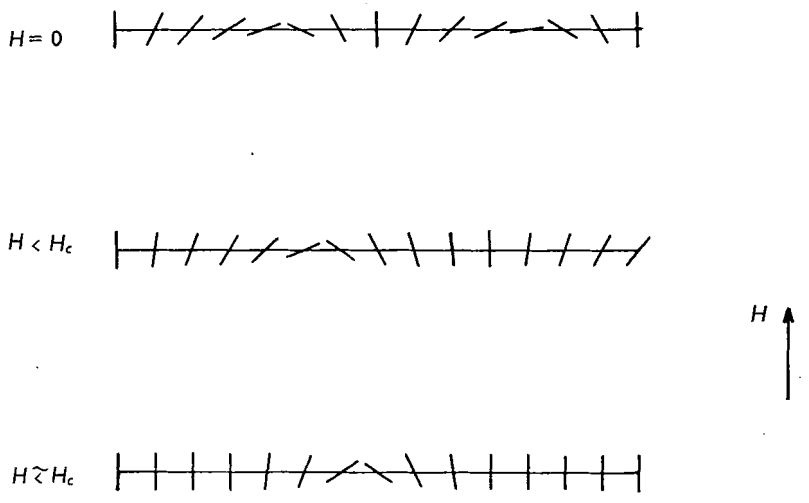

Figure 4. Configuration of a cholesteric liquid crystal under magnetic fields, when $\chi_{\parallel} - \chi_{\perp} > 0$ (conical structures neglected). (Perspective view.)

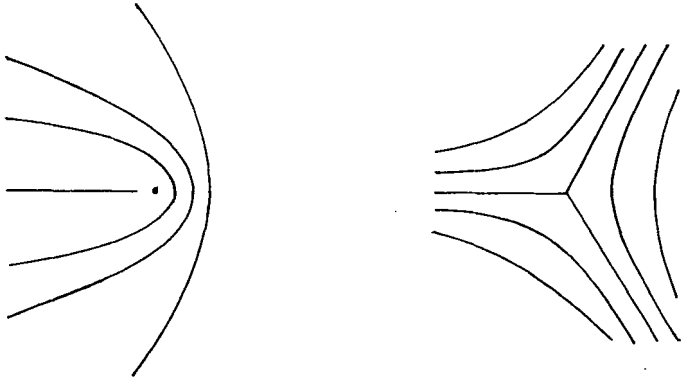

Figure 5. Two dimensional distortions in nematic crystals, leading to disclination lines (normal to the figure) of rank 1 (after Frank[1]).

(Note that at $H = H_c$, the coherence length is comparable to the pitch π/q_0 of the 0 field spiral.) Typical values of H_c may be in the 100 koe range, but H_c may be decreased by a suitable choice of q_0 (small q_0 or large pitch).

The plot of free energy vs H has no discontinuity in slope at

$H = H_c$. However it should be emphasized that at $H = H_c$, the nematic configuration is still stable with respect to all small amplitude deformations. The situation is reminiscent of a ferromagnetic ellipsoid in decreasing fields: when the demagnetization field balances exactly the external field, the completely aligned state is still completely stable with respect to spin waves (for a non 0 anisotropy field), but it is unstable with respect to Bloch walls (i.e. large amplitude deformations). In fact the structure shown on Fig. 4c for H just below H_c has some similarity with a Bloch wall.

One further complication has been pointed out by Meyer[11]: when the elastic constants satisfy a certain inequality:

$$\frac{\kappa_{22}}{\kappa_{33}} > \frac{\pi^2}{4} \tag{2.8}$$

a *conical* structure becomes stable at intermediate field values. This corresponds to:

$$n_x = \sin\theta\cos(qz)$$
$$n_y = \sin\theta\sin(qz)$$
$$n_z = \cos\theta$$

when z is an axis parallel to **H**, and θ is space independent. When condition (2.8) is satisfied, we expect the following succession of phases (in increasing fields):

distorted spiral (axis $\perp$ **H**) $\leftrightarrow$ conical (axis $\parallel$ **H**) $\leftrightarrow$ nematic

If condition (2.8) is *not* satisfied, we have the simpler scheme:

distorted spiral $\leftrightarrow$ nematic.

Experimental data on magnetic field effects in cholesteric crystals are few in number, but at least one cholesteric material becomes nematic under high fields (in the 100 koe range).[12] Clearly, it would be of interest to follow the transition by optical methods, measuring the pitch of the distorted spiral, etc.[12a]

3. Optical Striations in Small Angle Cholesteric Prisms

Possible discontinuities in the field $\mathbf{n}(\mathbf{r})$ have been discussed by Frank,[3] under the denomination of " disclination lines ". Typical cases considered by Frank are shown on Fig. 5. In the present section we wish to call attention on another class of disclination lines, occuring with cholesteric crystals under specific boundary conditions: the active material is inserted between two glass plates making a small angle (Fig. 6). The two plates are uni-

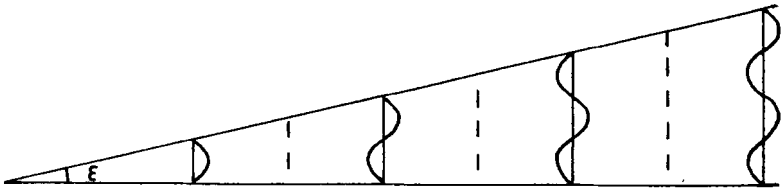

Figure 6. Conformation of cholesteric spirals in a small angle wedge. On the limiting planes, the molecular axis has an imposed direction, normal to the plane of the figure. The optical rotation for beams parallel to the spiral axis shows discontinuities at the locations marked by dotted lines.

axially polished and impose a fixed direction for $\mathbf{n}$ at their contact. When observed with an optical beam roughly normal to the plates, the liquid crystal exhibits, at the polarizing microscope, a succession of strips with different transmissions, the strips being separated by very sharp boundaries.

Forty-five years ago, G. Friedel[13] suggested that these boundaries correspond to discontinuities of the torsion in the cholesteric spiral. This has been proven in details by the optical studies of Cano.[14] On one side of the discontinuity the director $\mathbf{n}$ makes for instance half-turn between the two plates, while on the other side it makes a full turn, as shown on Fig. 6. How does the transition take place between the two types of behavior? There seem to be two possible answers:

(a) A *sheet* of discontinuity extending all the way from one plate to the other. This corresponds more or less to Cano's interpretation of his results.[14]

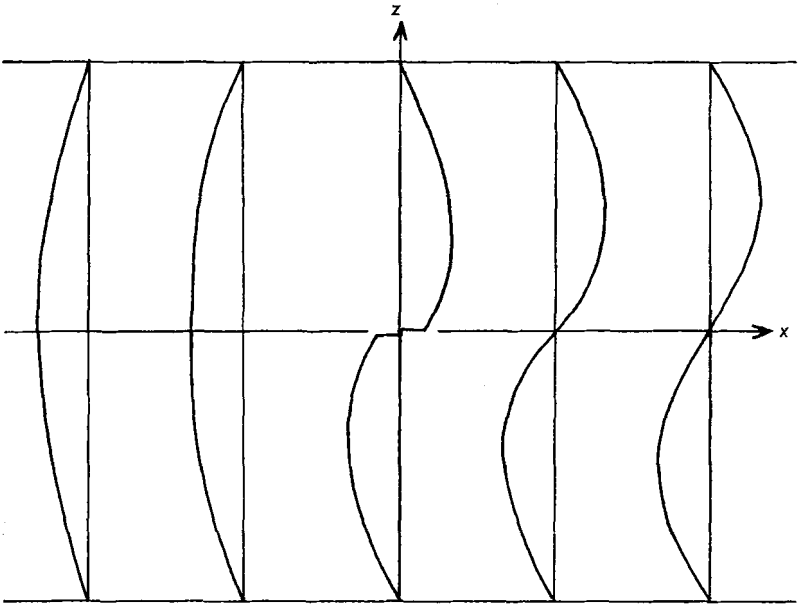

Figure 7. Possible structure of the molecular alignment near one discontinuity. The disclination line is normal to the plane of the figure. Molecules just above (below) the line make an angle of $+45°$ ($-45°$) with the plane of the figure.

(b) A *line* of discontinuity, parallel to the plates and lying halfway between them.[15] Comparison with similar problems in other branches of physics (vortices in helium, dislocations . . .) suggest that the line solution is energetically less expensive. One structure for such a postulated line is shown on Fig. 7. The vector **n** is constantly in the plane of the plates:[15a]

$$\left.\begin{aligned} n_x &= \cos\phi(x, z) \\ n_y &= \sin\phi(x, z) \\ n_z &= 0 \end{aligned}\right\} \qquad (3.1)$$

where $0z$ is the direction normal to the plates (in the transition region we may neglect completely the small angle ϵ between

them). The angle ϕ defining the local direction of the director is a smooth function of x and z, except on the singular line ($x = z = 0$). In the vicinity of the line we have:

$$\phi = \text{const} + q_0 z + \tfrac{1}{2} \tan^{-1}(z/x) \tag{3.2}$$

Eq. (3.2) in this simplified form is correct only when the three elastic constants are equal, but the general structure remains valid in all cases.‡ The line corresponds to $x = 0$, $z = 0$ (i.e., coincides with the y axis). The discontinuity in ϕ appears most clearly if we move in the mid-plane of the slab (the xy plane). In the region $x > 0$, on one side of the line, $\phi = 0$ (dropping the constant term in Eq. (3.2)). On the other side ($x < 0$) another determination of the $\tan^{-1}$ function comes into play, and $\phi = \pm \pi/2$. More generally, in three dimensional space, if we follow an arbitrary closed path encircling once the y axis, we find that ϕ is increased (or decreased) by π. The director $\mathbf{n}(\mathrm{r})$ is thus a double valued function of r, with two opposite determinations: but since $\mathbf{n}$ and $-\mathbf{n}$ are physically equivalent the state at point $\mathbf{r}$ is still defined unambiguously. The increment $|\Delta\phi| = \pi$ is the smallest (non zero) value satisfying this requirement, and corresponds to a disclination line of rank 1 in Frank's classification.[3]

On the molecular scale, the line will have a core, of size comparable to the molecular diameter a; this core cannot be detected directly with an optical microscope: this explains why the discontinuities observed by Cano[14] are so sharp.

To conclude: this configuration with a small angle prism between polished plates allows to produce disclination lines in a strictly controlled fashion. A number of experiments on the interactions and motions of these lines should be feasible.[15b] Also, to study the core, one might add a droplet of soluble dye in the slab: the dye should diffuse more rapidly along the cores, and this could be followed optically.

‡ The main effect of unequal elastic constants is to give a line energy which becomes dependent on the angle between the line and the preferred direction imposed by polishing of the plates.

4. Thermal Fluctuations of the Orientation

1. Fluctuations and Correlations in a Nematic Crystal

We restrict our attention to *long wavelength* fluctuations of the orientation in a nematic single crystal.[16] The average orientation of the crystal (defined by a director $\mathbf{n}_0$, parallel to the z axis) may be imposed either by contact with uniaxially polished walls, or by a magnetic field H, parallel to $0z$ (assuming that $\chi_a > 0$). The fluctuations are described by small, non-zero components $n_x(\mathbf{r})$, $n_y(\mathbf{r})$. To second order in n_x and n_y the free energy defined in Eqs. (1.2), (1.3) becomes:

$$f - f_0 = \frac{1}{2}\int d\mathbf{r}\left\{\kappa_{11}\left(\frac{\partial n_x}{\partial x} + \frac{\partial n_y}{\partial y}\right)^2 + \kappa_{22}\left(\frac{\partial n_x}{\partial y} - \frac{\partial n_y}{\partial x}\right)^2 + \kappa_{33}\left[\left(\frac{\partial n_x}{\partial z}\right)^2 + \left(\frac{\partial n_y}{\partial z}\right)^2\right] + \chi_a H^2(n_x^2 + n_y^2)\right\} \tag{4.1}$$

It is convenient to analyze n_x and n_y in Fourier components, defined by

$$n_x(\mathbf{k}) = \int d\mathbf{r}\, n_x(\mathbf{r})\, e^{i\mathbf{k}\cdot\mathbf{r}}\,, \text{ etc.} \ldots \tag{4.2}$$

In terms of these Fourier components $\mathscr{F}$ becomes

$$\mathscr{F} - \mathscr{F}_0 = \frac{1}{2}\Omega^{-1}\sum_{k}\left[\kappa_{11}\left| k_x n_x(\mathbf{k}) + k_y n_y(\mathbf{k})\right|^2 + \kappa_{22}\left| k_x n_y(\mathbf{k}) - k_y n_x(\mathbf{k})\right|^2 + (\kappa_{33}q_z^2 + \chi_a H^2)(\left| n_x(\mathbf{k})\right|^2 + \left| n_y(\mathbf{k})\right|^2)\right] \tag{4.3}$$

where Ω is the sample volume. For a given $\mathbf{k}$, it is convenient to diagonalize the quadratic form in Eq. (4.2) by a suitable choice of axes (Fig. 8). We introduce for each $\mathbf{k}$ two unit vectors $\mathbf{e}_1$ and $\mathbf{e}_2$; $\mathbf{e}_1$ is normal to $\mathbf{k}$ and to $\mathbf{n}_0$; $\mathbf{e}_2$ is normal to $\mathbf{n}_0$ and to $\mathbf{e}_1$. In terms of these vectors we may write $\mathbf{k} = \mathbf{n}_0 k_z + \mathbf{e}_1 k_\perp$. The component of $\mathbf{n}(\mathbf{k})$ along $\mathbf{e}_\alpha$ will be written $\mathbf{n}_\alpha(\mathbf{k})$. Then we obtain

$$f - f_0 = \frac{1}{2}\Omega^{-1}\sum_{k}\sum_{\alpha=1,2}\left| n_\alpha(\mathbf{k})\right|^2\left[\kappa_{33}k_\parallel^2 + \kappa_{\alpha\alpha}k_\perp^2 + \chi_a H^2\right] \tag{4.4}$$

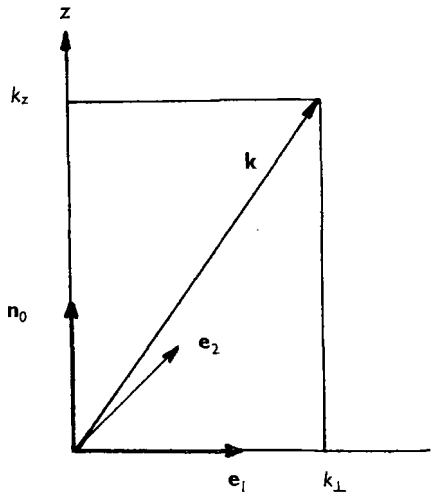

Figure 8. Definition of the unit vectors $\mathbf{e}_1$ and $\mathbf{e}_2$ which specify the fluctuation modes of given wave vector k in a nematic crystal aligned along z.

In Eq. (4.4) the various degrees of freedom $n_\alpha(\mathbf{k})$ are decoupled. We can now derive the thermal average of $|\, n_\alpha(\mathbf{k})\,|^2$ simply from the equipartition theorem

$$\langle\, |\, n_\alpha(\mathbf{k})\,|^2 \,\rangle = \Omega k_B T \frac{1}{\kappa_{33} k_z^2 + \kappa_{\alpha\alpha} k_\perp^2 + \chi_a H^2} \tag{4.5}$$

(The equipartition theorem holds only in the classical limit, namely when $\hbar\omega_\alpha(\mathbf{k}) \ll k_B T$, where $\omega_\alpha(\mathbf{k})$ is a characteristic frequency for the mode $(\alpha, \mathbf{k})$. A detailed analysis of the motions[17] shows that this requirement is satisfied when both the wavelength $2\pi/k$ and the magnetic coherence length ξ are much larger than a, i.e. when we are in the range of validity of the continuum model.)

It is of interest to derive first from Eq. (4.5) the spatial dependence of the correlation functions between values of $\mathbf{n}$ measured at two different points $\mathbf{r}$ and $\mathbf{r}'$. This calculation is particularly simple and illuminating when all elastic constants are equal $\kappa_{11} = \kappa_{22} = \kappa_{33} = \kappa$. In this case we may write

$$\langle\, |\, n_x(\mathbf{k})\,|^2 \,\rangle = \langle\, |\, n_y(\mathbf{k})\,|^2 \,\rangle = \frac{\Omega k_B T}{K(k^2 + \xi^{-2}} \tag{4.6}$$

$$\langle n_x(\mathbf{r})n_x(\mathbf{r}')\rangle = \langle n_y(\mathbf{r})n_y(\mathbf{r}')\rangle = \Omega^{-1}(2\pi)^{-3}\int d_3k\langle \mid n_x(\mathbf{k})\mid^2\rangle e^{i\mathbf{k}\cdot\mathbf{R}}$$

$$= \frac{k_BT}{4\pi KR}\exp(-R/\xi) \qquad (4.7)$$

$(\mathbf{R} = \mathbf{r} - \mathbf{r}')$

Eq. (4.7) supplements our discussion of section 1 on the significance of the coherence length ξ: we see that ξ is the range of the correlation of $\mathbf{n}$. When the magnetic field tend to 0, the correlation becomes a slowly decreasing function of R (namely R^{-1}). In the more realistic case where the three constants κ_{ii} are different, the correlation functions can also be written down, but they become more complex. In all cases, however, the qualitative conclusions drawn above remain valid.

2. Scattering of Light by Thermal Fluctuations

The propagation of light is sensitive to fluctuations in the dielectric tensor $\hat{\epsilon}$. Neglecting all magneto–optic effects, and assuming that the medium has no natural optical activity, the most general form for $\hat{\epsilon}$ at a given point $\mathbf{r}$ is

$$\hat{\epsilon}(\mathbf{r}) = \bar{\epsilon} + \epsilon_a(\mathbf{n}:\mathbf{n} - 1/3) \qquad (4.8)$$

Thus $\hat{\epsilon}$ is modulated by the fluctuations of $\mathbf{n}$. The density fluctuations in the liquid may also play a rôle (they modulate both $\bar{\epsilon}$ and ϵ_a). But we shall see that the fluctuations of $\mathbf{n}$ are in fact the dominant effect.

Consider an ingoing beam of wave vector $\mathbf{k}_0$, polarization vector $\mathbf{i}$, frequency ω, and an outgoing beam ($\mathbf{k}_1$, $\mathbf{f}$, $\omega' \cong \omega$). The analysis is particularly simple if $\epsilon_a \ll \bar{\epsilon}$ since in this case both beams can be considered to propagate in an isotropic medium. Thus in all that follows we assume $\epsilon_a \ll \bar{\epsilon}$.

Then the differential cross section σ_d for scattering from $\mathbf{k}_0$ to $\mathbf{k}$, is given by:

$$\sigma_d = \pi^2\lambda^{-4}\langle \mid \mathbf{f}\cdot\hat{\epsilon}(\mathbf{k})\cdot\mathbf{i}\mid^2\rangle \qquad (4.9)$$

where λ is the wavelength in the vacuum ($\lambda = (2\pi C)/\omega$) and

$\mathbf{k} = \mathbf{k}_0 - \mathbf{k}$ is the scattering vector. $\hat{\epsilon}(\mathbf{k})$ is the Fourier transform of $\hat{\epsilon}(\mathbf{r})$ defined as in Eq. (4.2) (with this definition σ_d is proportional to the volume of scattering material). A derivation of Eq. (4.9) is given in the appendix.

We now restrict our attention to the contributions in $\hat{\epsilon}(\mathbf{k})$ which are due to the fluctuations of $\mathbf{n}$. Let us write

$$\mathbf{n} = \mathbf{n}_0 + \delta\mathbf{n}$$

where $\delta\mathbf{n}$ has the components $(n_x, n_y, 0)$. We expand the anisotropic part of $\hat{\epsilon}$ in powers of $\delta\mathbf{n}$. The terms of order 0 are space independent and do not contribute to the Fourier transform for $k \neq 0$. The terms of first order yield:

$$\mathbf{f} \cdot \hat{\epsilon}(\mathbf{k}) \cdot \mathbf{i} = \epsilon_a(\delta\mathbf{n}(\mathbf{k}) \cdot \mathbf{i}(\mathbf{k}_0 \cdot \mathbf{f}) + (\delta\mathbf{n}(\mathbf{k}) \cdot \mathbf{f})(\mathbf{n}_0 \cdot \mathbf{i})$$

For a given $\mathbf{k}$ we analyse $\delta\mathbf{n}$ in terms of the two unit vectors $\mathbf{e}_1\,\mathbf{e}_2$ defined above $\delta\mathbf{n} = n_1\mathbf{e}_1 + n_2\mathbf{e}_2$. The average square amplitudes of $n_1(\mathbf{k})$ and $n_2(\mathbf{k})$ have been computed (Eq. (4.5)) and there are no cross terms between n_1 and n_2. This leads to a differential cross section (per unit volume)

$$\frac{\sigma_d}{\Omega} = \left(\frac{\epsilon_a\omega^2}{4\pi C^2}\right)^2 \Omega^{-1} \langle \mid n_1(\mathbf{k}) \mid^2 \rangle (i_1 f_z + i_z f_1)^2 + \langle \mid n_2(\mathbf{k}) \mid^2 \rangle (i_2 f_z + f_2 i_z) \qquad (4.10)$$

$(i_\alpha \equiv \mathbf{e}_\alpha \cdot \mathbf{i}, \quad f_\alpha \equiv \mathbf{e}_\alpha \cdot f)$

Let us discuss first the *order of magnitude* of this cross section. Consider a case where all elastic constants are equal and $H = 0$. Then from Eq. (4.5) we find

$$\frac{\sigma_d}{\Omega} \sim \left(\frac{\epsilon_a\omega^2}{4\pi C^2}\right)^2 \frac{k_B T}{K k^2} \qquad (4.11)$$

We shall compare this with the cross section σ'_d for scattering by density fluctuations. A local dilatation $\theta(\mathbf{r})$ has similar effects on $\bar{\epsilon}$ and ϵ_a: for simplicity we shall take into account only the modulation of $\bar{\epsilon}$

$$\bar{\epsilon}(\mathbf{r}) = \bar{\epsilon}_0 + \epsilon'\theta(\mathbf{r}) \qquad (4.12)$$

The corresponding cross section, derived from Eq. (4.11), is

$$\sigma'_d = \left(\frac{\epsilon'\omega^2}{4\pi C^2}\right)^2 (\mathbf{f}\cdot\mathbf{i}) \langle \mid \theta(\mathbf{k}) \mid^2 \rangle \tag{4.13}$$

To derive the thermal average $\langle \mid \theta(\mathbf{k}) \mid^2 \rangle$ we use the compressional free energy $\mathscr{F}_c$ in the form

$$\mathscr{F}_c = \frac{1}{2}\int d\mathbf{r}\, U\theta^2(r) = \frac{1}{2}\Omega^{-1}U\sum_k \mid \theta(\mathbf{k}) \mid^2 \tag{4.14}$$

where U^{-1} is an isothermal compressibility.

Applying the equipartition theorem (which is correct for the long wavelengths under consideration) we find a k independent result:

$$\langle \mid \theta(\mathbf{k}) \mid^2 \rangle = \Omega\frac{k_BT}{U} \qquad \frac{\sigma'_d}{\Omega} = \left(\frac{\epsilon'\omega^2}{4\pi C^2}\right)(\mathbf{f}\cdot\mathbf{i})^2\frac{k_BT}{U} \tag{4.15}$$

For an order of magnitude estimate we may put $\epsilon' \sim 1$ and $\epsilon_a \sim 1$. Also $K \sim Ua^2$ where a is a molecular diameter. Then, comparing (4.11) and (4.15) we see that

$$\frac{\sigma_d}{\sigma'_d} \sim \frac{1}{(ka)^2}$$

Since k^{-1} is an optical wavelength (or even larger if we consider small angle scattering), σ_d is considerably larger than σ'_d: the fluctuations of $\mathbf{n}$ dominate the scattering behavior. This observation explains the apparent turbidity of nematic single crystals, as compared to isotropic liquids. The difference in polarization factors between (4.10) and (4.15) also explains why the scattered light is strongly depolarized.[7]

Let us now turn to a discussion of the information which can be obtained from detailed scattering measurements. Usually absolute values of cross sections are not measured; but, by a suitable choice of the scattering geometry, one can extract from the data the thermal averages $\langle \mid n_\alpha(\mathbf{k}) \mid \rangle^2$, except for a constant scale factor:

(a) For experiments in 0 magnetic field, we expect from Eq. (4.5) that $\langle \mid n_\alpha(\mathbf{k}) \mid^2 \rangle$ be inversely proportional to $\kappa_{33}k_z^2 + \kappa_{\alpha\alpha}k_\perp^2$. This leads to a very strong scattering at small angles (where $k \to 0$). This analytic dependence appears to be in reasonable agreement with the data of Châtelain.[16] Comparing data at different values k_z and $k_\perp$ one should be able to extract the ratios $\kappa_{\alpha\alpha}/\kappa_{33}$.

(b) With a strong field H, the fluctuations $\langle \mid n_\alpha(\mathbf{k}) \mid^2 \rangle$ become inversely proportional to $\kappa_{33}k_z^2 + \kappa_{\alpha\alpha}k_\perp^2 + \chi_\alpha H^2$. The scattering intensity at small angles is reduced. If χ_α is measured by a separate experiment, it is now possible to *measure the three elastic constants* directly. It is greatly to be hoped that such experiments will be carried out in the near future.

In practice, there is one slight complication due to the fact that ϵ_a is not necessarily small in comparison with $\bar{\epsilon}$: the light beams propagate in a uniaxial medium, and all intensity formula must be accordingly refined. But, independently of these technical details, it is clear that light scattering studies will play an important role for the determination of elastic coefficients in nematic (or cholesteric) materials.

Another interesting possibility is to analyze the *frequency spectrum* of the outgoing light, for a very monochromatic (laser) source: from this one can extract detailed informations on coupled rotational and hydrodynamic motions in liquid crystals. The basic equations of motion for this problem have been laid down by Eriksen[18] and Leslie.[19] The resulting motions for $n_\alpha(\mathbf{k})$ are strongly damped oscillations.[17] Experimental measurements of the power spectrum of $n_\alpha(\mathbf{k})$ should allow for a clear cut determination of the viscosity and coupling parameters in liquid crystals.

Acknowledgments

The author is greatly indebted to J. Billard, R. Cano, P. Châtelain, G. Durand, J. Friedel, R. Meyer, G. Sarma, J. Villain, for various conversations and written exchanges of views on the physics of liquid crystals.

Appendix

DERIVATION OF EQ. (4.7)

The starting point is the formula for radiation emission by a dipole **P** oscillating at the frequency ω, and located at point **r**:

$$\mathbf{E}(\mathbf{r}') = \frac{\omega^2}{C^2 R} e^{ik_1 R} \mathbf{P}_\perp(\mathbf{r}) \qquad \mathbf{R} = \mathbf{r}' - \mathbf{r} \tag{A. 1}$$

where $\mathbf{P}_\perp$ is the component of **P** normal to the direction of observation. We write that the dipoles **P** are due to the ingoing field

$$\mathbf{E}_{in}(\mathbf{r}) = \mathbf{i}\, e^{i\mathbf{k}_0 \cdot \mathbf{r}}$$

$$\mathbf{P}(\mathbf{r}) = \frac{1}{4\pi}\left[\hat{\epsilon}(\mathbf{r}) - 1\right]\mathbf{E}_{in}(\mathbf{r}) \tag{A. 2}$$

The outgoing field $\mathbf{E}_{\text{out}}$ is obtained by an integration over the scattering volume Ω

$$\mathbf{E}_{\text{out}}(\mathbf{r}) = \frac{\omega^2}{4\pi C^2 R}\int_\Omega d\mathbf{r}\left\{\left[\hat{\epsilon}(\mathbf{r}) = \mathbf{1}\right]\mathbf{i}\right\}_\perp e^{i(\mathbf{k}_0 - \mathbf{k}_1)\cdot \mathbf{r}} \tag{A. 3}$$

(where R is assumed to be large, and all constant phase factors have been omitted). We introduced the scattering wave vector $\mathbf{k} = \mathbf{k}_0 - \mathbf{k}$ and project $\mathbf{E}_{\text{out}}$ on the polarization direction **f** (**f** is normal to $\mathbf{k}_\perp$). The scattering amplitude is the coefficient of $1/R$ in this expression and the differential cross section σ^d is the thermal average of the squared amplitude

$$\sigma^d = \left[\frac{\omega^2}{4\pi C^2}\right]^2 \langle \left| \mathbf{f} \cdot \hat{\epsilon}(\mathbf{k}) \cdot \mathbf{i} \right|^2 \rangle \tag{A. 4}$$

(the term -1 in $\hat{\epsilon} - 1$ drops out for $\mathbf{k} \neq 0$).

REFERENCES

1. Oseen, C. W., *Trans. Faraday Soc.* **29**, 883 (1933).
2. Zocher, H., *Trans. Faraday Soc.* **29**, 945 (1933).
3. Frank, F. C., *Disc. Faraday Soc.* **25**, 1 (1958). See also Eriksen, J. L., *Arch. Rational Mech. Anal.* **10**, 189, 1962.
4. Electric fields could also be used in principle, but their effects are usually dominated by impurity conduction.

5. Frederiks, V., Zolina, V., *Zh. RF. Kharkov* **59**, 183 (1927); *Trans-Faraday Soc.* **29**, 919 (1933).
5a. Calculations of the Frederiks transition allowing for unequal elastic constants, flexible boundary conditions, etc., have been carried out recently: see Pincus, P., Papoular, M. and Rapini, A., *Compt. Rend. Acad. Sc. Paris*, **267**, 1230 (1968).
Rapini, A., *Compt. Rend. Acad. Sc. Paris* (to be published).
6. Grandjean, F., *Compt. Rend. Acad. Sc. Paris* **172**, 71 (1921).
7. Châtelain, P., *Acta Crystallographica* **1**, 315 (1948).
8. Yoshimori, A., *Journ. Phys. Soc. Japan* **14**, 807 (1959).
Villain, J., *Phys. Chem. Sol.* **11**, 303 (1959).
9. Meyer, R. B., *Applied Phys. Lett.* **12**, 281 (1968).
10. De Gennes, P. G., *Solid State Comm.* **6**, 163 (1968).
11. Meyer, R. B., private communication. Conical configurations were dismissed in ref 10 on the basis of a calculation which assumed all elastic constants to be equal.
12. Sakmann, E., Meiboom, S., Snyder, L. C., *Journ. Am. Chem. Soc.* **89**, 5981 (1967).
12a. This has been carried out recently: see Durand, G., Leger, L., Rondelez, F. and Veyssie, M., *Phys. Rev. Lett.* **22**, 227 (1969).
13. Friedel, G., *Ann. de Phys.* **2**, No. 18, p. 273 (1922).
14. Cano, R., *Bull. Soc. Minéralogie Cristallographie* **91**, 20 (1968).
15. De Gennes, P. G., *Compt. Rend. Acad. Sc. Paris* **266**, 571 (1968).
15a. Caroli, C. and Dubois-Violette, E. have shown that n_z is not strictly 0 in the exact solution for this type of line; however n_z is small at distances $r < q_0^{-1}$ from the line.
15b. More recent experiments and other models for the discontinuities have been presented: Orsay Liquid Crystals Group, *Physics Letters* **28A**, 687 (1969).
16. De Gennes, P. G., *Compt. Rend. Acad. Sc. Paris* **266**, 15 (1968).
17. A detailed analysis of the damped oscillations is submitted for publication in the *Journ. Chem. Phys.*
18. Eriksen, J. L., *Arch. Rational Mech. Anal.* **23**, 266 (1966).
19. Leslie, F. M., *Arch. Rational Mech. Anal.* **28**, 256 (1968).